Identification and characterization of an *Arabidopsis* mutant with altered localization of NIP5;1, a plasma membrane boric acid channel, reveals the requirement for D-galactose in endomembrane organization

Running head:

Endomembrane organization is dependent on D-galactose

Corresponding author:

Dr. J. Takano

Graduate School of Agriculture, Hokkaido University, Kita-ku N9-W9, Sapporo 060-8589, Japan

Tel: +81-11(706)3888, FAX: +81-11(706)4932, Email: jtakano@abs.agr.hokudai.ac.jp

Subject area:

Special Focus Issues: Plant Endomembranes.

Membrane and transport

Number of black and white figures: 1, Color figures: 6, Supplementary figures: 4, Supplementary tables: 2

Title

Identification and characterization of an Arabidopsis mutant with altered localization of NIP5;1, a plasma membrane boric acid channel, reveals the requirement for D-galactose in endomembrane organization

Running Head

Endomembrane organization is dependent on D-galactose

Authors

Masataka Uehara[1], Sheliang Wang[1], Takehiro Kamiya[2], Shuji Shigenobu[3], Katsushi Yamaguchi[3], Toru Fujiwara[2], Satoshi Naito[1,4], Junpei Takano[1]

[1] Graduate School of Agriculture, Hokkaido University, Sapporo 060-8589, Japan

[2] Graduate School of Agricultural and Life Science, The University of Tokyo, Tokyo 113-8657, Japan

[3] National Institute for Basic Biology, Okazaki 444-8585, Japan

[4] Graduate School of Life Science, Hokkaido University, Sapporo 060-0810, Japan

Abbreviations: ACC, 1-aminocyclopropane-1-carboxylic acid; AGP, arabinogalactan-protein;

40 B, boron; DIC, differential interference contrast; DMSO, dimethyl sulfoxide; EMS,
41 ethylmethane sulfonate; ER, endoplasmic reticulum; GFP, green fluorescent protein; KAM,
42 katamari; MVB, multivesicular body; NIP, nodulin 26-like intrinsic protein; PM, plasma
43 membrane; REB, root epidermal bulgar; RG, rhamnogalacturonan; RHD, root hair defective;
44 SNP, single nucleotide polymorphism; SSLP, simple sequence length polymorphism; TGN,
45 *trans*-Golgi network; UGE, UDP-D-glucose-4-epimerase; XXT, xylosyltransferase
46
47 **Abstract**
48 Endomembrane organization is important for various aspects of cell physiology, including
49 membrane protein trafficking. To explore the molecular mechanisms regulating the
50 trafficking of plasma membrane-localized proteins in plants, we screened for *Arabidopsis*
51 mutants with defective localization of GFP-NIP5;1. Fluorescence imaging-based screening
52 led to the isolation of a mutant, which accumulated abnormal intracellular aggregates labeled
53 by GFP-NIP5;1. The aggregates appeared in epidermal cells in the root elongation zone and
54 included the *trans*-Golgi network/early endosomes. Rough mapping and whole-genome
55 sequencing identified the mutant as an allele of *UDP-glucose 4-epimerase (uge) 4/root hair*
56 *defective (rhd) 1/root epidermal bulgar (reb) 1*, which was originally defined as a cell wall
57 mutant. The responsible gene encodes UDP-glucose 4-epimerase 4 (UGE4), which
58 functions in the biosynthesis of D-galactose, especially for the synthesis of the cell wall

polysaccharide xyloglucan and arabinogalactan proteins (AGPs). The endomembrane aggregates in the mutants were absent in the presence of D-galactose, indicative of a requirement for a D-galactose-containing component in endomembrane organization. Genetic and pharmacological analyses suggested that the aggregates were not caused by the disruption of cell wall polysaccharides or the cytoskeleton. Overall, our results suggest that UGE4 activity in D-galactose synthesis is required for the structure of cell wall polysaccharides and endomembrane organization.

Key words: *Arabidopsis thaliana*, cell wall, endomembrane, D-galactose, UDP-D-glucose-4-epimerase

Introduction

Membrane trafficking between endomembranes and the plasma membrane (PM) plays an important role in plant cells. Membrane proteins destined for the PM are inserted into the endoplasmic reticulum (ER) membrane, transported through Golgi stacks and the *trans*-Golgi network (TGN), and are then targeted to the PM. Increasing numbers of PM-localized proteins show polar localization in specific PM domains, possibly through different secretion and recycling pathways (Park and Jürgens 2012, Löfke et al. 2012). PM-localized proteins are selectively or non-selectively transported to early endosomes by endocytosis. It is now accepted that the TGN functions as an early endosome in plant cells, and thus serves as a major sorting hub for the secretory and endocytic pathways (Viotti et al. 2010, Uemura et al. 2012). From the TGN/early endosomes, membrane proteins can be recycled back to the PM or proceed to multivesicular bodies (MVBs)/late endosomes. At the limiting membrane of MVBs, the membrane proteins destined for degradation are transported to luminal vesicles (Spitzer et al. 2009, Viotti et al. 2010). MVBs fuse with vacuoles and release their luminal vesicles into the lumen of a lytic vacuole, where the proteins are degraded by proteases (Scheuring et al. 2011).

The structural organization of the endomembrane is important for proper membrane trafficking and is fundamental for plant physiology. Previously, a fluorescence imaging-based screen using a transgenic *Arabidopsis thaliana* line expressing vacuole-targeted green fluorescent protein (GFP) identified the *katamari* (*kam*) mutants,

which contain endomembrane aggregates in their cells (Tamura et al. 2005, 2007). The interaction between KAM1, a Golgi membrane protein, with actin filaments was shown to be important for proper endomembrane organization. Another screen using a polar PM marker *ProPIN1:PIN1-GFP* identified the *protein-affected trafficking2 and 4* (*pat2* and *pat4*) mutants, which showed strong intracellular accumulation of PIN1-GFP (Feraru et al. 2010, Zwiewka et al. 2011). In these mutants, the morphology and function of lytic and protein storage vacuoles are defective and membrane proteins accumulate in the aberrant vacuolar structures. Map-based cloning identified *PAT2* and *PAT4* as putative β and δ subunits of the adaptor protein-3 complex, and suggested that the plant adaptor protein-3 complex plays a role in mediating lytic vacuole performance and in the transition of storage into lytic vacuoles. These studies indicate that the fluorescence imaging-based screening of *Arabidopsis* mutants can be used to identify important components of endomembrane organization.

In this study, to explore the mechanisms regulating membrane trafficking and endomembrane organization in plant cells, we screened *Arabidopsis* mutants with a defect in the localization of GFP-nodulin 26-like intrinsic protein (NIP)5;1 using fluorescence microscopy. NIP5;1 is a PM-localized boric acid channel belonging to the major intrinsic protein (aquaporin) family (Takano et al. 2006). NIP5;1 plays a role in boric acid uptake and is required for the normal growth of *Arabidopsis* plants under low boron (B) conditions (Takano et al. 2006). NIP5;1 is localized to the PM of root cap cells and root epidermal cells

110 with polarity toward the outer (soil-facing) side of the cells (Takano et al. 2010). The
111 polarity of NIP5;1 is thought to be associated with the limited lateral diffusion in the PM, but
112 the mechanisms for polar trafficking and retention remain unclear. Here, we report the
113 isolation of a mutant that accumulated endomembrane aggregates labeled by GFP-NIP5;1.
114 We identified the mutant as a novel allele of *UDP-D-glucose 4-epimerase (uge) 4/root hair*
115 *defective (rhd) 1/root epidermal bulgar (reb) 1*, which was isolated as mutants of root hair
116 development, root morphology, and susceptibility to nematodes (Schiefelbein and Somerville
117 1990, Baskin et al. 1992, Baum et al. 2000). UGE4 activity in D-galactose synthesis is
118 required for the structure of cell wall polysaccharides (Ding and Zhu 1997, Andème-Onzighi
119 et al. 2002, Seifert et al. 2002, Nguema-Ona et al. 2006, Rösti et al. 2007). In this study, we
120 demonstrate that UGE4 is also required for endomembrane organization, which is important
121 for the proper localization of membrane proteins.
122
123 **Results**
124 **Screening for mutants with altered localization of GFP-NIP5;1 identified mutants with**
125 **intracellular aggregates**
126 To identify novel factors involved in regulating the intracellular localization of
127 NIP5;1, we performed fluorescence imaging-based screening to obtain mutants in which
128 NIP5;1 was localized abnormally in cells. For this purpose, we used transgenic *Arabidopsis*

129 harboring *ProNIP5;1 (Δ5'UTR)::GFP-NIP5;1* as a transgene in the *nip5;1-1* mutant. In the
130 construct, we used the NIP5;1 promoter lacking the 5'UTR of *NIP5;1*, which is responsible
131 for the B-dependent degradation of *NIP5;1* mRNA, to obtain relatively strong expression of
132 GFP-NIP5;1 irrespective of the B level (Tanaka et al. 2011). In the transgenic plants,
133 GFP-NIP5;1 localized to the PM in root epidermal cells (Fig. 1A-C and Takano et al. 2010).
134 For screening, approximately 25,000 GFP-NIP5;1 seeds were mutagenized with ethylmethane
135 sulfonate (EMS), and 20 pools of M2 seeds were obtained. We screened ~40,000 M2 seeds
136 from the 20 pools under fluorescence microscopes and isolated 17 mutant lines in which
137 GFP-NIP5;1 showed aberrant localization. Among them, three mutants showed localization
138 of GFP-NIP5;1 in intracellular aggregates. In this study, we focused on Line 20-2, in which
139 GFP-NIP5;1 was often localized to abnormal intracellular aggregates in epidermal cells in the
140 root elongation zone (Fig. 1A). These aggregates were also observed in epidermal cells in
141 the root hair zone, but not in the root meristem zone (Supplementary Fig. S1A). In the
142 mutant elongation zone, bulging of the epidermal cells started to appear, leading to swelling
143 of the cells in the root hair zone (Fig. 1A). A cross-section of the elongation zone showed
144 that the aggregates accumulated in trichoblasts (root hair-forming cells), which are in contact
145 with two cortical cells, and in atrichoblasts, which are in contact with only one cortical cell
146 (Fig. 1C). The polar localization of GFP-NIP5;1 in the plasma membrane was not affected
147 in epidermal cells containing aggregates (Fig. 1D).

148 Since intracellular trafficking pathways could have been disturbed, we stained the
149 root cells with a lipophilic styryl dye (FM4-64) to examine the endocytic pathway. In
150 wild-type (WT) epidermal cells, FM4-64 stained dotty endosomes within 30 min (Fig. 1D).
151 However, in the epidermal cells of Line 20-2, FM4-64 stained aggregates containing
152 GFP-NIP5;1 (Fig. 1D). These results suggest that the intracellular structure labeled with
153 GFP-NIP5;1 contained membranes in the endocytic pathway. The use of FM4-64 also
154 revealed that the aggregates were absent from leaf epidermal cells (Supplementary Fig. S1B).
155
156 **Rough mapping and genome sequencing identified Line 20-2 as a novel allele of the *uge4***
157 **mutant**
158 To identify the gene responsible for Line 20-2, we performed genetic mapping and
159 whole-genome sequencing. We outcrossed the mutant (Col-0 background) with L*er* plants
160 and analyzed the phenotypes of F_2 plants. Among 117 F_2 plants, 28 contained aggregates
161 with GFP-NIP5;1, indicating that the phenotype was caused by a single recessive mutation
162 ($p=0.79$ by a X^2 test). Genotyping using the 28 F_2 plants with 11 simple sequence length
163 polymorphism (SSLP) markers roughly mapped the mutation to a region between 13.8 and 27
164 Mb on chromosome 1 (Fig. 2A, Supplementary Table S1).
165 We performed whole-genome sequencing of Line 20-2 on the SOLiD platform
166 (Applied Biosystems). Sequence libraries were constructed from Line 20-2 and another

three mutants obtained from the same screen. The read sequences were mapped to the *A. thaliana* Col-0 genome. Nine nucleotide changes were found in the exons of the genetically mapped region (between 13.8 and 27 Mb on chromosome 1) after subtracting shared single nucleotide polymorphisms (SNPs) among the four mutant lines, which could be originally present in the parental transgenic line. Of the 9 mutations, 7 were G/C-to-A/T transitions, which are known to arise from the EMS-mediated alkylation of guanine and adenine. Annotation of these 7 EMS-induced mutations indicated that 4 were nonsynonymous, 1 was nonsense, and the rest were silent (Supplementary Table S2). The one nonsense mutation was in the gene AT1G64780 while the nonsynonymous mutations were found in AT1G56570, AT1G64440, AT1G72950, and AT1G73160 (Fig. 2A).

In the candidate genes for the causative mutations, we identified *UGE4/RHD1/REB1* (At1g64440), whose loss-of-function mutants showed similar root bulging phenotypes to Line 20-2 (Schiefelbein and Somerville 1990, Baskin et al. 1992). Line 20-2 had a single mutation (G1365A) in *UGE4/RHD1/REB1*, which resulted in the replacement of Gly^{223} (GGA) with Arg (AGA) (Fig. 2A, Supplementary Table S2). To determine whether Line 20-2 is an allele of the *uge4* mutant, we first stained roots of *rhd1-1* and SALK_080766, a T-DNA insertion allele of *uge4* (Fig. 2A) with FM4-64 (Fig. 2B). In both alleles, FM4-64 stained aggregates in elongating epidermal cells, as in Line 20-2 (Fig. 1D). F_1 plants between Line 20-2 and *rhd1-1* or SALK_080766 were then produced and their roots were

186 stained with FM4-64. The roots of the F_1 plants contained aggregates stained by FM4-64
187 and contained GFP-NIP5;1 (Fig. 2C). These results indicated that Line20-2 is allelic to the
188 *uge4* mutant.
189
190 **Abnormal intracellular aggregates contain TGN/early endosomes**
191 Since the GFP-NIP5;1-labeled aggregates were stained with FM4-64, an endocytic
192 tracer, we assumed that the structure contained endomembranes along the endocytic pathway.
193 As expected, significant amounts of two TGN/early endosome markers, YFP-VTI12 and
194 YFP-RabA1e (Geldner et al. 2009), were localized to the aggregates using FM4-64 in the
195 *uge4* (SALK_080766) mutant (Fig. 3A). We then stained the ER using ER tracker Red (Fig.
196 3B). In the cells with GFP-NIP5;1-labeled aggregates, ER tracker Red stained network
197 structures, including the aggregates, suggesting that part of the ER membrane was included in
198 the aggregates. Differential interference contrast (DIC) images showed apparently normal
199 vacuolar structures in the cells containing aggregates (Fig. 1B). These observations
200 suggested that some (but not all) of the endomembrane accumulated in the aggregates.
201 We then performed time-course analysis of FM4-64 uptake to investigate the
202 endocytic pathway from PM to vacuolar membranes in *uge4* mutants. In both wild-type and
203 the *uge4* mutant, FM4-64 was observed as dotty structures after staining for 5 min, suggesting
204 that endocytosis of FM4-64 from the plasma membrane was not impaired in the mutant (Fig.

4A). However, FM4-64 showed stained aggregates after 15 min, and the intensity of FM4-64 in the aggregates increased after 30 min in the *uge4* mutant (Fig. 4A). After 160 min, FM4-64 clearly stained the vacuolar membrane in wild-type cells; however, the staining was less intense in the *uge4* mutant (Fig. 4B). These results suggested that the *uge4* mutant had a defect in the later endocytic pathway from TGN/early endosomes to vacuoles.

Intracellular aggregates were absent after D-galactose and ethylene-precursor treatment in *uge4*

UGE4 encodes an isoform of UDP-D-glucose-4-epimerase, which interconverts UDP-D-glucose and UDP-D-galactose and is involved in D-galactose synthesis (Seifert et al. 2002). In *uge4*, the D-galactose content is decreased and the bulging of epidermal cells is rescued by the addition of D-galactose to the growth medium (Seifert et al. 2002). Thus, we grew our mutant in the presence of 10 mM D-galactose and found that D-galactose rescued the bulging and decreased endomembrane aggregation in epidermal cells (Fig. 5). This result indicated that D-galactose synthesized by UGE4 is required for endomembrane organization in epidermal cells of the root elongation zone. We next explored whether D-galactose decreased the number of existing aggregates. Based on our time-course analysis, 10 mM D-galactose did not affect existing aggregates within 110 min in the elongation zone (Supplementary Fig. S2A). After 19 h in the presence of D-galactose, aggregates were still

observed in the epidermal cells in the root hair zone, but not in the elongation zone (Supplementary Fig. S2A). These results indicated that the external addition of D-galactose decreased the appearance of aggregates, but did not affect existing aggregates.

Previous reports have shown that root epidermal bulging in *rhd1* is suppressed by ethylene or its precursor 1-aminocyclopropane-1-carboxylic acid (ACC) (Seifert *et al*. 2004). The authors proposed that ethylene signaling channels UDP-D-galactose to specific UDP-D-galactose requiring molecules. Therefore, we investigated whether ACC also suppressed aggregate formation. In epidermal cells after 5 μM ACC treatment for 2 days, the bulging and aggregates were not observed in Line 20-2 (Supplementary Fig. S3). This result suggested that ethylene increased the transfer of UDP-D-galactose synthesized by alternative UGE isoforms to a D-galactose-containing molecule required for endomembrane organization.

Intracellular aggregates in *uge4* mutants differ from the structures caused by cytoskeleton disruption

Cortical microtubules are either disordered or absent in the enlarged trichoblasts of *uge4* plants (Andème-Onzighi et al. 2002). To investigate the involvement of the cytoskeleton in endomembrane aggregation, we performed pharmacological inhibition of the assembly of actin and microtubules using latrunculin B and oryzalin, respectively, in

243 transgenic WT plants expressing GFP-NIP5;1 (Fig. 6). Interestingly, both treatments
244 promoted the accumulation of GFP-NIP5;1 in spherical structures that differed from the
245 aggregates observed in the *uge4* mutants (Fig. 6A-E, compared to Fig. 1B, D). For
246 microtubule disruption, bulging was observed in epidermal cells of the elongation zone (Fig.
247 6C). These results suggest that cytoskeletal disruption causes endomembrane disorganization
248 and affects the trafficking of GFP-NIP5;1, but that the effect differs in *uge4* mutants.
249
250 **Genetic and pharmacological disturbances of cell wall polysaccharides did not induce**
251 **endomembrane aggregates**
252 D-galactose is a component of glycoproteins, glycolipids, and cell wall polysaccharides in
253 plant cells. Previous reports indicated that *uge4* mutants contained reduced amounts of
254 D-galactose, xyloglucan, and arabinogalactan proteins (AGPs), while pectin was not affected
255 (Ding and Zhu 1997, Andème-Onzighi et al. 2002, Seifert et al. 2002, Nguema-Ona et al.
256 2006). To explore whether the reduced amount of xyloglucan or AGPs causes
257 endomembrane aggregation, we analyzed *Arabidopsis* mutants with a low AGP or xyloglucan
258 content. In the roots of the *mur1* mutants, the L-fucose content was reduced by 40% (Reiter
259 et al. 1993), the content of fucosylated xyloglucan reactive to the monoclonal antibody
260 CCRC-M1 was significantly reduced (Freshour et al. 2003), and fucosylated AGPs were
261 decreased by 40% (van Hengel and Roberts 2002). The *mur1* mutation decreased root cell

elongation by ~50% and caused swelling at the base of the root hairs (van Hengel and Roberts 2002). In both *mur1-1* and *mur1-2* mutant plants, FM4-64 stained the PM and dotty endosomes, similar to wild type (Fig. 7A). This clearly differed from *uge4* (SALK_080766), in which the aggregates were stained. These results suggest that the defect in root elongation in the *mur1* mutants was not linked to endomembrane disorganization. We then used the *mur2* mutant, which contained less than 2% of the WT level of fucosylated xyloglucan in its cell wall (although the growth and wall strength were normal) (Vanzin *et al*. 2002), and the *xylosyltransferase (xxt) 1/xxt2* mutant, which contained no detectable xyloglucan and showed aberrant root hairs (Cavalier et al. 2008). FM4-64 stained the PM and dotty endosomes in these mutants, suggesting that xyloglucan is not required for endomembrane organization (Fig. 7A). To increase our understanding of AGPs, we treated plant roots with β-D-glucosyl Yariv reagent, a synthetic phenylglycoside that specifically binds AGPs (Yariv et al. 1967, Nguema-Ona et al. 2012). As reported, treatment with 10 μM Yariv reagent for 7 days phenocopied the epidermal bulging seen in *uge4* (Ding and Zhu 1997 and Fig. 7B). However, Yariv reagent did not induce endomembrane aggregates with GFP-NIP5;1 or FM4-64 in WT plants (Fig. 7B), suggesting that the cell bulging caused by AGP dysfunction in the cell wall is not associated with endomembrane disorganization. To explore the possible additive effect of defects in cell wall polysaccharides and AGPs, we treated the *mur1-2*, *mur2-1*, and *xxt1/xxt2* mutants with Yariv reagent (Fig. 7B). In the mutants treated

281 with Yariv reagent, the FM4-64 staining patterns varied between independent plants, possibly
282 because of severe cell wall damage. However, aggregates typically observed in the *uge4*
283 mutants were not apparent. In *xxt1/xxt2* mutants treated with Yariv reagent, abnormal
284 structures were occasionally stained by FM4-64 (Supplementary Fig. S4). However, the
285 structures were smaller and apparently different in shape from the aggregates in the *uge4*
286 mutant. Although additional studies are required to clarify the effect of simultaneous defects
287 in xyloglucan and AGPs, the reduced xyloglucan or dysfunction of AGPs in the cell wall was
288 not likely the direct cause of endomembrane disorganization in *uge4*.
289
290 **Discussion**
291 In this study, we performed a forward genetic analysis using transgenic *Arabidopsis* plants
292 expressing GFP-NIP5;1. GFP-NIP5;1 is localized to the PM of epidermal and lateral root
293 cap cells with polarity toward the outer (soil-facing) side of the roots (Takano et al. 2010).
294 Our approach can be used to identify the mechanisms underlying the trafficking of
295 PM-localized proteins, including ER exit, secretion, polar targeting, endocytosis, and vacuolar
296 trafficking. We identified mutants in which GFP-NIP5;1 was localized to the ER, the
297 vacuolar membrane (our unpublished results), and intracellular aggregates (Fig. 1). Our data
298 indicate that mutants with intracellular aggregates are defective in general endodmembrane
299 organization rather than in NIP5;1-specific trafficking mechanisms. Identification of the

300 responsible gene led to re-discovery of the cell wall mutant *rhd1/reb1/uge4* as a mutant of
301 endomembrane organization.

302 Previously, the *Arabidopsis* mutant *kam1* was identified in a screen based on
303 vacuole-targeted GFP-2sc (Tamura et al. 2005). This mutant contains endomembrane
304 aggregates with various organelles in the perinuclear region of its cells. However, the
305 structure of the aggregates differed between *uge4* and *kam1*. In *kam1*, endosomes stained
306 with FM4-64 were a minor component of the aggregates (Tamura et al. 2005), while in *uge4*,
307 the entire aggregate stained with FM4-64 (Fig. 1D). KAM1 is a Golgi membrane protein
308 that interacts with actin filaments. This interaction, rather than its activity as a xyloglucan
309 galactosyltransferase, is responsible for proper endomembrane organization. When leaf
310 epidermal cells were treated with latrunculin B, an actin-depolymerizing reagent, GFP-2sc
311 accumulated in aggregates, similar to the *kam1* mutant (Tamura et al. 2005). However, in
312 root epidermal cells, latrunculin B induced the accumulation of GFP-NIP5;1 in spherical
313 structures (Fig. 6D), apparently different from the aggregates in *uge4*. Therefore, the
314 endomembrane aggregation likely differs in *kam1* and *uge4*. Interestingly, the disruption of
315 microtubules by oryzalin also resulted in GFP-NIP5;1 accumulation in spherical structures
316 (Fig. 6E). A previous report on *reb1-1* (*uge4*) mutants showed that the microtubules in the
317 swollen trichoblasts were either disordered or absent entirely, while they were apparently
318 normal in atrichoblasts (Andème-Onzighi et al. 2002). In our analysis, aggregation occurred

319 in both trichoblasts and atrichoblasts in *uge4* mutants (Fig. 1C). These observations suggest
320 that disorganization of actin and microtubules is not likely the cause of endomembrane
321 aggregation in *uge4*.

322 *UGE4* encodes an isoform of UGE, which functions in the biosynthesis of
323 UDP-D-galactose (Seifert et al. 2002). There are five isoforms of UGE with distinct
324 enzymatic properties, and only *UGE4* influenced plant growth when a single isoform was
325 mutated (Barber et al. 2006, Rösti et al. 2007). Among the five isoforms, *UGE1 and -4* are
326 expressed in the root elongation zone (Rösti et al. 2007, Barber et al. 2006). Both UGE1 and
327 -4 are present in the cytoplasm, whereas UGE4 is additionally enriched close to Golgi stacks
328 (Barber et al. 2006). The distinct enzymatic properties and intracellular localization would
329 explain the occurrence of endomembrane aggregates in the root elongation zone of single
330 *uge4* mutants (Fig. 1). In contrast, the absence of aggregates in cotyledon of the *uge4*
331 mutants (Supplementary Fig. S1B) may be due to the redundant expression of all five *UGE*
332 isoforms in leaves (Rösti et al. 2007).

333 Since D-galactose in the media reduced endomembrane aggregation (Fig. 5), the
334 reduced amount or improper delivery of UDP-D-galactose in the cell caused the aggregation.
335 UDP-D-galactose is a donor nucleotide sugar for the biosynthesis of cell wall polysaccharides,
336 including xyloglucan, rhamnogalacturonan (RG)-I and -II pectins, AGPs, and chloroplast
337 galactolipids (Reiter and Vanzin, 2001). However, our results do not support the

338 involvement of any known D-galactose-containing components in UGE4-dependent
339 endomembrane organization. It was suggested that UGE4 is not required for galactolipid
340 synthesis based on a thin layer chromatographic analysis of lipids from roots or cotyledons
341 (Seifert et al. 2002). It is also unlikely that *uge4* mutations affect the N-glycosylation of
342 glycoproteins, because in the N-glycans of most glycoproteins D-galactose exists as the
343 trisaccharide Galβ(1→3)[Fucα(1→4)]GlcNAc, a structure absent from the N-glycans of *A.*
344 *thaliana* (Fitchette et al. 1999). Among D-galactose-containing polysaccharides, AGPs and
345 xyloglucan (but not RG-I and -II pectins) are reduced in *uge4* mutants compared to wild type
346 (Ding and Zhu 1997, Andème-Onzighi et al. 2002, Seifert et al. 2002, Nguema-Ona et al.
347 2006). A structural analysis revealed no changes in the galactosylation of RG-I and -II in
348 *uge4* roots (Nguema-Ona et al. 2006). Therefore, we focused on the involvement of AGPs
349 and xyloglucan in endomembrane organization. When we treated WT plants with
350 β-D-glucosyl Yariv reagent, which reacts with AGPs, epidermal bulging occurred, in
351 agreement with previous results (Ding and Zhu 1997). However, endomembrane
352 aggregation was not observed (Fig. 7B). Therefore, the function of AGPs in the cell wall is
353 not linked to endomembrane organization. The involvement of xyloglucan was examined
354 using the *mur2* mutant, which contains less than 2% of the WT amount of fucosylated
355 xyloglucan (Vanzin *et al*. 2002), and the *xxt1/xxt2* mutant, which lacks detectable xyloglucan
356 (Cavalier *et al*. 2008). In these mutants, endomembrane aggregation was not observed (Fig.

7A). The treatment of *mur2-1* and *xxt1/xxt2* with β-D-glucosyl Yariv reagent also did not induce the typical aggregates observed in *uge4* plants, suggesting that neither AGPs nor xyloglucan in the cell wall is responsible for endomembrane organization. However, the binding of Yariv reagent to AGPs and the lack of fucosyltransferase (MUR2) or xylosyltransferase (XXT1/2) should affect AGPs and xyloglucan differently in the *uge4* mutant, in which the supply of D-galactose to AGPs and xyloglucan is reduced. Therefore, it is possible that the reduced synthesis of AGPs or altered structures of AGPs and/or xyloglucan cause endomembrane disorganization in *uge4*. It is also possible that there is an unknown D-galactose-containing component specifically required for endomembrane organization. The suppression of aggregates in the presence of the ethylene-precursor ACC (Supplementary Fig. S3), which is thought to modulate the transfer of UDP-D-galactose to specific D-galactose requiring components (Seifert et al. 2004), may increase our understanding of the mechanism of endomembrane aggregation in *uge4* mutants.

In conclusion, we isolated a mutant with abnormal endomembrane aggregates and identified the responsible gene as *uge4*, encoding an enzyme for D-galactose synthesis. UGE4 activity is required for proper cell wall structure and endomembrane organization.

Materials and Methods

Plant materials and growth conditions

Arabidopsis thaliana ecotype L*er* was obtained from our laboratory stocks.

ProNIP5;1 (-5'UTR)::GFP-NIP5;1 (Tanaka et al. 2011), Wave 13Y, 34Y (Geldner et al. 2009), and the *mur1* (Reiter et al. 1993), *mur2* (Reiter et al. 1997), and *xxt1/xxt2* (Park and Cosgrove 2012) mutants of *A. thaliana* were described previously. All plants were grown on vertically placed solid medium (Takano et al. 2005) containing 1% (w/v) sucrose, 1.5% (w/v) gellan gum, and 30 μM boric acid for 4-10 days in growth chambers at 22°C under fluorescent lamps with a 16-h/8-h light/dark cycle. For experiments with D-galactose, 10 mM D-galactose was added to the solid medium.

Mutant screening

For mutant screening, 25,000 T_4 seeds of GFP-NIP5;1 were mutagenized with 0.3% EMS for 17 h and 20 pools of M_2 seeds were obtained. M_2 seedlings grown on solid medium containing 30 μM boric acid for 7-10 days were observed under the epifluorescence microscope with a 20× dry lens (Leica HC PL APO CS), and candidates showing abnormal GFP-NIP5;1 localization were selected. At the beginning of the mutant selection process, we observed plants showing growth levels lower than wild type (10,000 plants/30,000 seeds). Half-way through the selection procedure, we examined the localization of GFP-NIP5;1 in every plant (10,000 seeds). We screened approximately 40,000 M_2 seeds and observed ~20,000 seedlings.

Genetic mapping

For genetic mapping, Line 20-2 (Col-0 background) was crossed with the L*er* ecotype and F_2 seeds were obtained. Genomic DNA was extracted from F_2 plants exhibiting the mutant phenotype of GFP-NIP5;1. For rough mapping, SSLP markers were used as follows: F14J9, F28J9, NGA280, and NGA111 for chromosome 1; T12J2 and NGA168 for chromosome 2; NGA162 and CIW4 for chromosome 3; NGA8 for chromosome 4; and MBK20 and K20J1 for chromosome 5 (Supplementary Table S1). We referred to the TAIR

403 marker database
404 (http://www.arabidopsis.org/servlets/Search?action=new_search&type=marker) and Cereon
405 database (http://www.arabidopsis.org/cereon/) in selecting our SSLPs.
406
407 **Whole-genome re-sequencing and data analysis**
408 Genomic DNA of an M_3 homozygous mutant was isolated using a DNeasy Plant
409 Mini Kit (Qiagen). Library construction and emulsion PCR were performed as described in
410 the SOLiD fragment library construction kit (Applied Biosystems). The libraries were
411 sequenced to 75 bp using the Applied Biosystems 5500xl SOLiD System with an Exact Call
412 Chemistry module.
413 Color space reads produced by the SOLiD sequencer were mapped to the *A. thaliana*
414 genome reference TAIR10 using LifeScope 2.1 software (Life Technologies) with default
415 parameters. SNPs were called using a diBayes SNP caller, a component of LifeScope.
416 diBayes was executed with a parameter setting defined as 'medium call stringency.'
417 Integrative Genomics Viewer (Robinson et al. 2011) was used to visualize the mapped reads
418 and called SNPs, along with gene models. To predict the functional impact of the SNPs, we
419 categorized them into coding (synonymous or non-synonymous), intronic, intergenic, and
420 splicing sites using custom scripts (Tabata et al. 2012). Gene models and the annotations
421 were based on TAIR10.
422
423 **Imaging analysis**
424 Laser scanning confocal microscopy was performed using Leica TCS SP5 and SP8
425 (equipped with an HC PL APO CS2 20× IMM lens and HCX PL APO CS 40×
426 water-immersion lens) with the following excitation and detection wavelengths: 488 and
427 500-530 or 500-550 nm for GFP; 488 and 500-540 nm for YFP; 488 and >640 nm long-pass
428 for FM4-64; and 552 and >600 nm long-pass for ER tracker Red. DIC was used to image

cell structures. FM4-64 (Molecular Probes) was prepared as a 10 mM stock solution in water and used at 4 μM for 5-160 min. ER tracker Red (Molecular Probes) was prepared as a 1 mM stock in dimethyl sulfoxide (DMSO) and used at 2 μM for 1 min and washed with water. To disrupt actin filaments or microtubules, latrunculin B or oryzalin was used, respectively, at 10 μM for 2 days. Latrunculin B and oryzalin (Wako Pure Chemicals) were prepared at 10 mM in DMSO. Plants were transferred from solid to liquid medium containing the dye or inhibitors and incubated at room temperature or in the growth chamber at 22°C, respectively. The liquid medium was replaced each day. Control treatments for the inhibitor experiments were performed with 0.2% DMSO. β-D-glucosyl Yariv reagent was dissolved in 0.15 M NaCl at 2 mg/ml as a stock solution. Plants were incubated in liquid medium containing 1.5 mM NaCl as a control experiment or 30 μM Yariv reagent for more than 20 h in a growth chamber at 22°C. The ethylene precursor 1-aminocyclopropane-1-carboxylic acid (ACC, Sigma) was prepared as a 10 mM stock solution in water and used at 5 μM in solid medium.

Funding

This work is supported by the NEXT program (to J. T.) and Grant-in-Aid for Scientific Research (Kiban S, to T.F.) from the Japanese Society for the Promotion of Science (JSPS).

Acknowledgements

We acknowledge Masahira Hattori and Kenshiro Oshima (University of Tokyo) for genome sequencing, Tomoko Shimizu and Kayo Konishi for technical assistance, and Shinji Wakuta and Akira Yoshinari for critical reading. We thank Mayuki Tanaka (University of Tokyo), Niko Geldner (University of Lausanne), Malcolm O'Neill (University of Georgia), and

Nottingham Arabidopsis Stock Centre and Arabidopsis Biological Resource Center for providing materials.

References

Andème-Onzighi, C., Sivaguru, M., Judy-March, J., Baskin, T.I. and Driouich, A. (2002) The *reb1-1* mutation of Arabidopsis alters the morphology of trichoblasts, the expression of arabinogalactan-proteins and the organization of cortical microtubules. *Planta* 215: 949–958.

Barber, C., Rösti, J., Rawat, A., Findlay, K., Roberts, K. and Seifert, G.J. (2006) Distinct properties of the five UDP-D-glucose/UDP-D-galactose 4-epimerase isoforms of Arabidopsis thaliana. *J. Biol. Chem.* 281: 17276–17285.

Baskin, T., Betzner, A., Hoggard, R., Cork, A. and Williamson, R.E. (1992) Root morphology mutants in *Arabidopsis thaliana*. *Aust. J. Plant Physiol*. 19: 427–437.

Baum, T.J., Wubben, M.J.E., Hardy,Y.K.A., Su, H. and Rodermel, S.R. (2000) A screen for *Arabidopsis thaliana* mutants with altered susceptibility to Heterodera schachtii. *J. Nematol* 32: 166–173.

Cavalier, D.M., Lerouxel, O., Neumetzler, L., Yamauchi, K., Reinecke, A., Freshour, G. et al. (2008) Disrupting two *Arabidopsis thaliana* xylosyltransferase genes results in plants deficient in xyloglucan, a major primary cell wall component. *Plant Cell* 20: 1519–1537.

Ding, L. and Zhu, J.K. (1997) A role for arabinogalactan-proteins in root epidermal cell expansion. *Planta* 203: 289–294.

Feraru, E., Paciorek, T., Feraru, M.I., Zwiewka, M., De Groodt, R., De Rycke, R. et al. (2010) The AP-3 β adaptin mediates the biogenesis and function of lytic vacuoles in Arabidopsis. *Plant Cell* 28: 12-24.

Fitchette, A.C., Cabanes-Macheteau, M., Marvin, L., Martin, B., Satiat-Jeunemaitre, B., Gomord, V. et al. (1999) Biosynthesis and immunolocalization of Lewis a-containing N-glycans in the plant cell. *Plant Physiol.* 121: 333–344.

Freshour, G., Bonin, C.P., Reiter, W.D., Albersheim, P., Darvill, A.G. and Hahn, M.G. (2003) Distribution of fucose-containing xyloglucans in cell walls of the *mur1* mutant of Arabidopsis. *Plant Physiol*. 131: 1602–1612.

Geldner, N., Dénervaud-Tendon, V., Hyman, D.L., Mayer, U., Stierhof, Y.D. and Chory, J. (2009) Rapid, combinatorial analysis of membrane compartments in intact plants with a multicolor marker set. *Plant J.* 59(1): 169–178.

Löfke, C., Luschnig, C. and Kleine-Vehn, J. (2012) Posttranslational modification and trafficking of PIN auxin efflux carriers. *Mech. Dev.*130(1): 1–13.

Nguema-Ona, E., Andème-Onzighi, C., Aboughe-Angone, S., Bardor, M., Ishii, T., Lerouge, P. et al. (2006) The *reb1-1* mutation of Arabidopsis. Effect on the structure and localization of galactose-containing cell wall polysaccharides. *Plant Physiol*. 140: 1406–1417.

Nguema-Ona, E., Coimbra, S., Vicré-Gibouin, M., Mollet, J.C. and Driouich, A. (2012) Arabinogalactan proteins in root and pollen-tube cells: distribution and functional aspects. *Ann. Bot.* 110(2): 383–404.

Park, M. and Jürgens, G. (2012) Membrane traffic and fusion at post-Golgi compartments. *Front. Plant Sci.* 2: 1–15.

Park, Y.B. and Cosgrove, D.J. (2012) Changes in cell wall biomechanical properties in the xyloglucan-deficient *xxt1/xxt2* mutant of Arabidopsis. *Plant Physiol.*158: 465–475.

Reiter, W.D., Chapple, C.C. and Somerville, C.R. (1993) Altered growth and cell walls in a fucose-deficient mutant of Arabidopsis. *Science* 261: 1032–1035.

Reiter, W.D., Chapple, C. and Somerville, C.R. (1997) Mutants of *Arabidopsis thaliana* with altered cell wall polysaccharide composition. *Plant J.* 12: 335–345.

Reiter, W.D. and Vanzin, G.F. (2001) Molecular genetics of nucleotide sugar interconversion pathways in plants. *Plant Mol. Biol.* 47: 95–113.

Robinson, J., Thorvaldsdóttir, H., Wendy, W., Mitchell, G., Eric, S.L., Gad, G. et al. (2011) Integrative genomics viewer. *Nat. Biotechnol.* 29(1): 24–26.

Rösti, J., Barton, C.J., Albrecht, S., Dupree, P., Pauly, M., Findlay, K. et al. (2007) UDP-glucose 4-epimerase isoforms UGE2 and UGE4 cooperate in providing UDP-galactose for cell wall biosynthesis and growth of *Arabidopsis thaliana*. *Plant Cell* 19: 1565–1579.

Scheuring, D., Viotti, C., Krüger, F., Künzl, F., Sturm, S., Bubeck, J. et al. (2011) Multivesicular bodies mature from the trans-Golgi network/early endosome in Arabidopsis. *Plant Cell* 23: 3463–3481.

Schiefelbein, J. and Somerville, C. (1990) Genetic control of root hair development in *Arabidopsis thaliana*. *Plant Cell* 2: 235–243.

Seifert, G.J., Barber, C., Wells, B., Dolan, L., and Roberts, K. (2002) Galactose biosynthesis in Arabidopsis: genetic evidence for substrate channeling from UDP-D-galactose into cell wall polymers. *Current Biol.* 12: 1840–1845.

Seifert, G.J., Barber, C., Wells, B. and Roberts, K. (2004) Growth Regulators and the Control of Nucleotide Sugar Flux. *Plant Cell* 16: 723–730.

Spitzer, C., Reyes, F.C., Buono, R., Sliwinski, M.K., Haas, T.J. and Otegui, M.S. (2009) The ESCRT-related CHMP1A and B proteins mediate multivesicular body sorting of auxin carriers in Arabidopsis and are required for plant development. *Plant Cell* 21: 749–766.

Tabata, R., Kamiya, T., Shigenobu, S., Yamaguchi, K., Yamada, M., Hasebe, M. et al. (2012) Identification of an EMS-induced causal mutation in a gene required for boron-mediated root development by low-coverage genome re-sequencing in Arabidopsis. *Plant Signal Behav*. 8(1): e22534.

Takano, J., Miwa, K., Yuan, L., von Wirén, N. and Fujiwara, T. (2005) Endocytosis and degradation of BOR1, a boron transporter of *Arabidopsis thaliana*, regulated by boron availability. *Proc. Natl. Acad. Sci. USA* 102: 12276–12281.

Takano, J., Wada, M., Ludewig, U., Schaaf, G., von Wirén, N. and Fujiwara, T. (2006) The Arabidopsis major intrinsic protein NIP5;1 is essential for efficient boron uptake and plant

development under boron limitation. *Plant Cell* 18: 1498–1509.

Takano, J., Tanaka, M., Toyoda, A., Miwa, K., Kasai, K., Fuji, K. et al. (2010) Polar localization and degradation of Arabidopsis boron transporters through distinct trafficking pathways. *Proc. Natl. Acad. Sci. USA* 107: 5220–5225.

Tamura, K., Shimada, T., Kondo, M., Nishimura, M. and Hara-Nishimura, I. (2005) KATAMARI1/MURUS3 is a novel golgi membrane protein that is required for endomembrane organization in Arabidopsis. *Plant Cell* 17: 1764–1776.

Tamura, K., Takahashi, H., Kunieda, T., Fuji, K., Shimada, T., and Hara-Nishimura, I. (2007). Arabidopsis KAM2/GRV2 is required for proper endosome formation and functions in vacuolar sorting and determination of the embryo growth axis. *Plant Cell* 19: 320–332.

Tanaka, M., Takano, J., Chiba, Y., Lombardo, F., Ogasawara, Y., Onouchi, H. et al. (2011) Boron-dependent degradation of NIP5;1 mRNA for acclimation to excess boron conditions in Arabidopsis. *Plant Cell* 23: 1–14.

Uemura, T., Kim, H., Saito, C., Ebine, K., Ueda, T., Schulze-lefert, P. et al. (2012). Qa-SNAREs localized to the trans -Golgi network regulate multiple transport pathways and extracellular disease resistance in plants. *Proc. Natl. Acad. Sci. USA* 109(5): 1784–1789.

van Hengel, A.J. and Roberts, K. (2002) Fucosylated arabinogalactan-proteins are required for full root cell elongation in arabidopsis. *Plant J.* 32: 105–113.

Vanzin, G.F., Madson, M., Carpita, N.C., Raikhel, N. V., Keegstra, K. and Reiter, W.D.

583 (2002) The *mur2* mutant of *Arabidopsis thaliana* lacks fucosylated xyloglucan because of a
584 lesion in fucosyltransferase AtFUT1. *Proc. Natl. Acad. Sci. USA* 99(5): 3340–3335.
585
586 Viotti, C., Bubeck, J., Stierhof, Y.D., Krebs, M., Langhans, M., van den Berg, W. et al.
587 (2010) Endocytic and secretory traffic in Arabidopsis merge in the trans-golgi network/early
588 endosome, an independent and highly dynamic organelle. *Plant Cell* 22: 1344–1357.
589
590 Yariv, J., Lis, H. and Katchalski, E. (1967) Precipitation of arabic acid and some seed
591 polysaccharides by glycosylphenylazo dyes. *Biochem. J.*105: 1c-2c
592
593 Zwiewka, M., Feraru, E., Möller, B., Hwang, I., Feraru, M.I., Kleine-Vehn, J. et al. (2011)
594 The AP-3 adaptor complex is required for vacuolar function in Arabidopsis. *Cell Res*. 21:
595 1–12.
596
597
598 **Figure legends**
599 Fig. 1. GFP-NIP5;1 in Line 20-2 accumulated in abnormal intracellular aggregates.
600 (A, B) GFP-NIP5;1 in the roots of WT plants and Line 20-2. The root meristem and
601 elongation zones (A), elongation zone (B), and cross-sections of the elongation zone (C) are
602 shown. (D) Polar localization of GFP-NIP5;1 in WT plants and Line 20-2. GFP-NIP5;1
603 showed polar localization toward soil-side in PM in comparison to FM4-64, which stained the
604 PM in a non-polar manner. Plants were grown on solid medium containing 30 μM boric
605 acid for 7-10 days. Roots were incubated with 4 μM FM4-64 for 30 min (D). *: trichoblast.
606 Bars = 50 μm (A), 10 μm (B, D), and 20 μm (C).
607
608 Fig. 2. Rough mapping and genome sequencing revealed that Line 20-2 is allelic to

609 *uge4/rhd1/reb1*. (A) Procedure for the identification of the responsible gene in Line 20-2
610 and the structure of *uge4/rhd1/reb1* (At1g64440), which has 9 exons. (B, C)
611 FM4-64-stained epidermal cells from the root elongation zone of *rhd1-1* and SALK_080766
612 plants (B) and F_1 plants from a cross between Line 20-2 and SALK080766 or *rhd1-1* (C).
613 Plants were grown on solid medium containing 30 μM boric acid for 7-10 days. Roots were
614 incubated with 4 μM FM4-64 for 30 min. Bars = 10 μm.
615
616 Fig. 3. The intracellular aggregates include the TGN.
617 (A) TGN markers, YFP-RabA1e (Wave34Y) and YFP-VTI12 (Wave13Y), in the epidermal
618 cells of WT and SALK_080766 plants. Plant roots were stained with FM4-64 for 30-40 min.
619 (B) ER tracker Red staining of epidermal cells from Line 20-2. Roots were incubated with 2
620 μM ER tracker Red for 1 min, washed with water, and then observed. Bars = 10 μm.
621
622 Fig. 4. The later endocytic pathway from TGN/early endosome to the vacuole is affected in
623 the *uge4* mutant.
624 (A, B) Time-course analysis of FM4-64 internalization in WT plants and Line 20-2 for 5, 15,
625 30 (A), and 160 min (B). Roots were stained with 4 μM FM4-64, washed with water, and
626 then observed after the indicated times. Bars = 10 μm.
627
628 Fig. 5. The intracellular aggregates in Line 20-2 were absent in the presence of D-galactose.
629 GFP-NIP5;1 in root elongation zones of WT plants and Line 20-2 grown on solid medium
630 containing 0 or 10 mM D-galactose (+D-gal) for 5 days. Bars = 20 μm.
631
632 Fig. 6. Intact actin filaments and microtubules are required for the organization of
633 endomembranes. GFP-NIP5;1 in root epidermal cells of WT plants incubated in liquid
634 medium containing 1% sucrose and 0.2% DMSO (control, A), 10 μM latrunculin B (B, D), or

10 μM oryzalin (C, E) for 2 days. Bars = 10 μm.

Fig. 7. A lack of xyloglucan and AGP dysfunction did not induce endomembrane aggregation. (A) FM4-64-stained roots of WT, *mur1-1*, *mur1-2*, *mur2-1*, and *xxt1/xxt2* plants. Note that in a cell in SALK_080766, vacuolar membranes were stained. This is probably because of direct penetrance by FM4-64 due to disruption of the PM. (B) GFP-NIP5;1 localization and FM4-64 staining pattern in roots of WT, *mur1-2*, *mu2-1*, and *xxt1/xxt2* plants treated with Yariv reagent. Plants were incubated in liquid medium containing 30 μM β-D-glucosyl Yariv reagent for more than 20 h and then stained with 4 μM FM4-64 for 30 min. Control treatment was performed with 1.5 mM NaCl. Bars = 10 μm.

Figure legends for supplementary figures

Supplementary Fig. S1

Aggregates were observed in epidermal cells in the root hair zone, but not in the leaves, of Line 20-2. A) In epidermal cells of the root hair zone, GFP-NIP5;1 was localized in the aggregates. Note that the signal of GFP-NIP5;1 on the PM was low in this area. White arrows indicate the aggregates. B) No aggregate stained with FM4-64 in the epidermal cells of cotyledon in both the WT and Line 20-2. Plant leaves were stained with 4 μM FM4-64 for 30 min. Bars = 100 μm.

Supplementary Fig. S2

The presence of 10 mM D-galactose did not affect existing aggregates. (A) The aggregates (indicated by arrows) remained evident after 110 min.

(B) The aggregates remained evident in epidermal cells in root hair zone, while they were not observed in the root elongation zone after 19 h in the presence of D-galactose. Bars = (A)

661 20 μm and (B) 50 μm.

662

663 Supplementary Fig. S3

664 Ethylene precursor 1-aminocyclopropane-1-carboxylic acid (ACC) treatment rescued the
665 aggregates. Five-day-old seedlings of Line 20-2 were transferred to solid medium containing
666 30 μM boric acid (Control) or 30 μM boric acid and 5 μM ACC for 2 days. Bars = 10 μm.

667

668 Supplementary Fig. S4

669 The abnormal structures observed in some of the roots of the *xxt1/xxt2* mutant treated with
670 Yariv reagent. The plants were treated with 30 μM β-D-glucosyl for 24 h and then stained
671 with 4 μM FM4-64 for 30 min (A-C). Enlarged images with FM4-64 and DIC are shown in
672 the right panels. In some of the abnormal structures, single spots with high intensity were
673 observed (A and B, indicated by white arrows). Bars = 10 μm.

Fig. 1

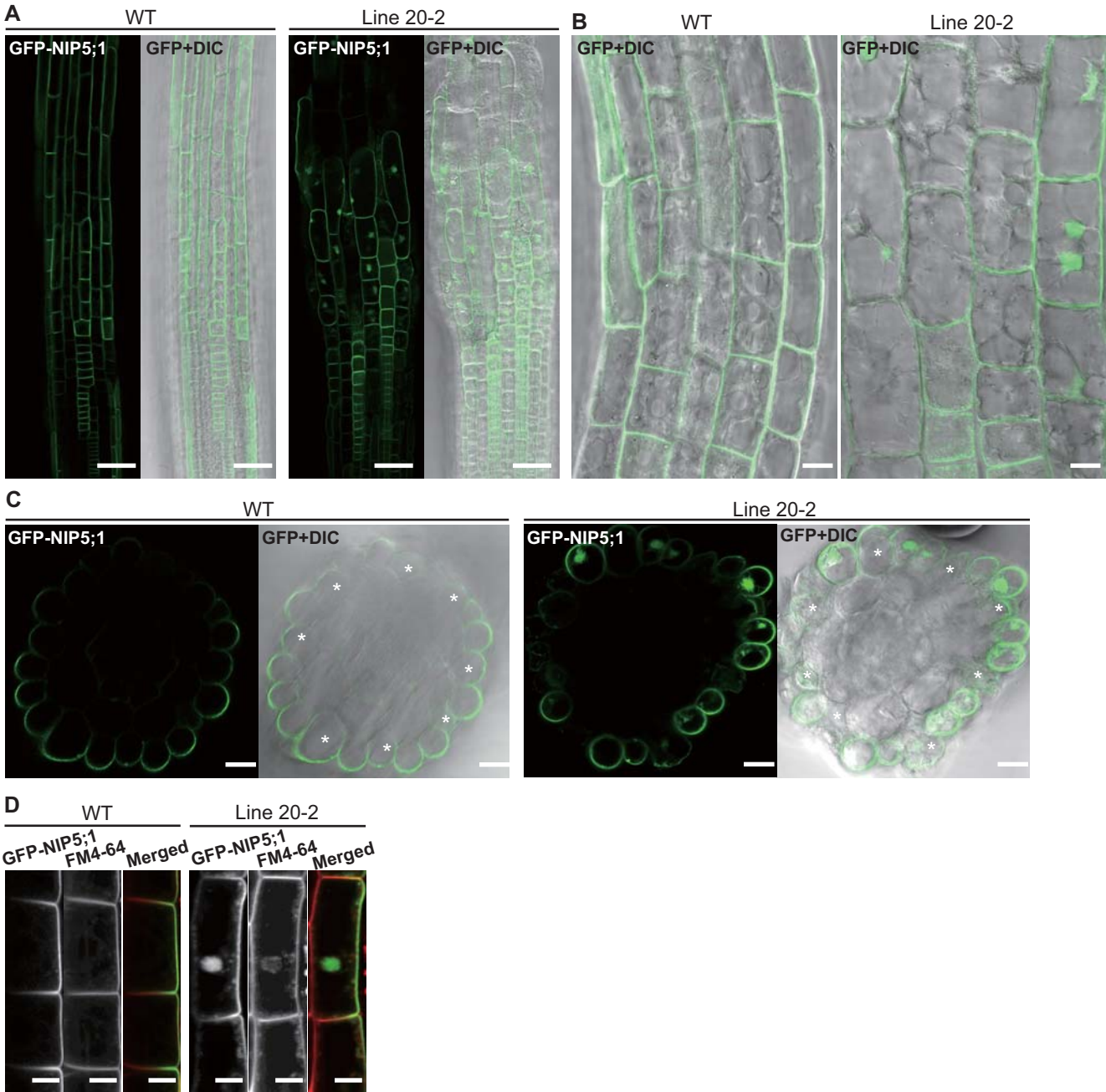
A
WT
Line 20-2
GFP-NIP5;1
GFP+DIC
GFP-NIP5;1
GFP+DIC
B
WT
Line 20-2
GFP+DIC
GFP+DIC
C
WT
Line 20-2
GFP-NIP5;1
GFP+DIC
GFP-NIP5;1
GFP+DIC
D
WT
Line 20-2
GFP-NIP5;1
FM4-64
Merged
GFP-NIP5;1
FM4-64
Merged

Fig. 2

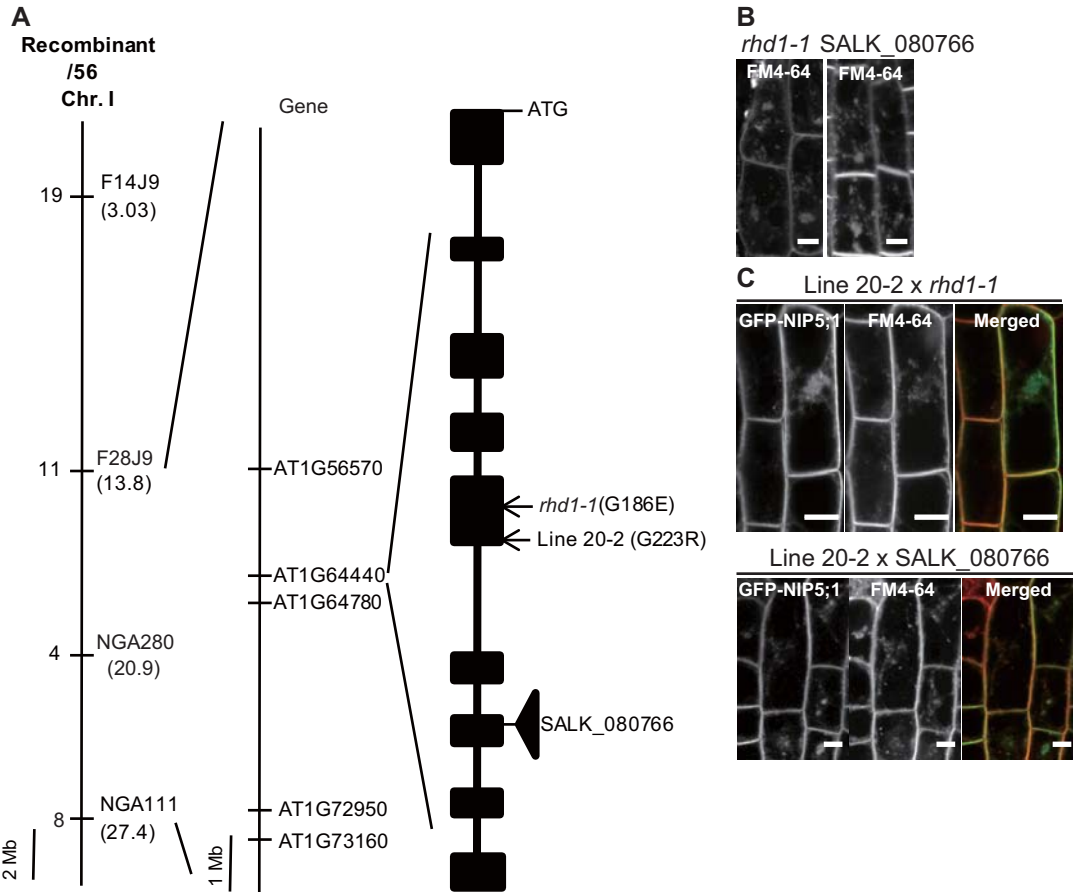
A
Recombinant
/56
Chr. I
Gene
ATG
19
F14J9
(3.03)
11
F28J9
(13.8)
AT1G56570
rhd1-1(G186E)
Line 20-2 (G223R)
AT1G64440
AT1G64780
4
NGA280
(20.9)
SALK_080766
8
NGA111
(27.4)
AT1G72950
AT1G73160
2 Mb
1 Mb
B
rhd1-1 SALK_080766
FM4-64
FM4-64
C
Line 20-2 x rhd1-1
GFP-NIP5;1
FM4-64
Merged
Line 20-2 x SALK_080766
GFP-NIP5;1
FM4-64
Merged

Fig. 3

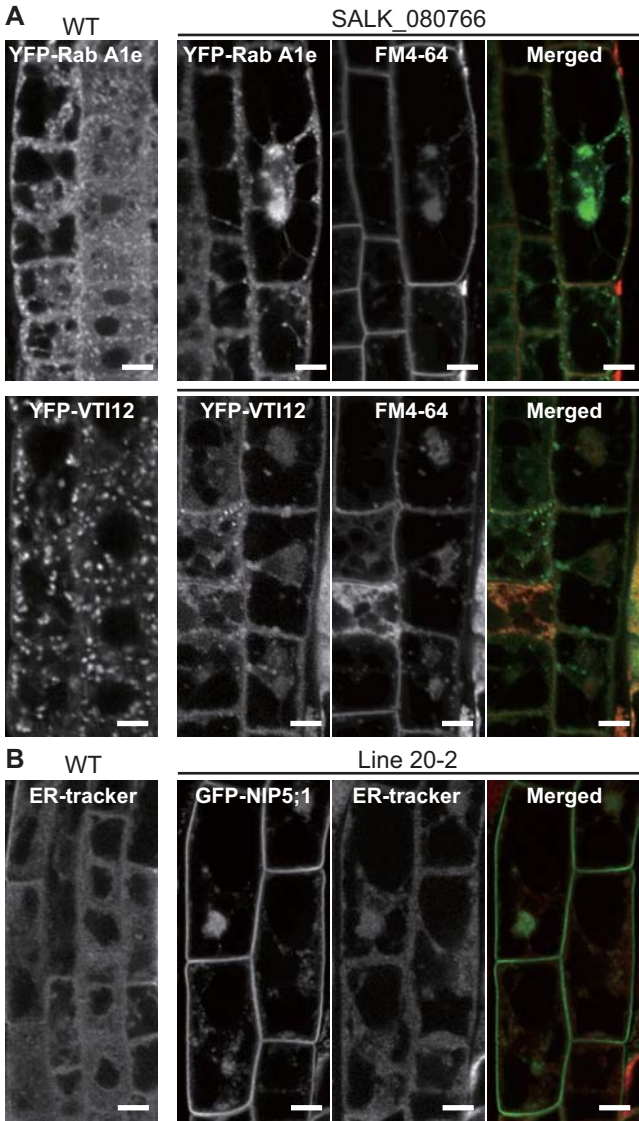
A
WT
SALK_080766
YFP-Rab A1e
YFP-Rab A1e
FM4-64
Merged
YFP-VTI12
YFP-VTI12
FM4-64
Merged
B
WT
Line 20-2
ER-tracker
GFP-NIP5;1
ER-tracker
Merged

Fig. 4

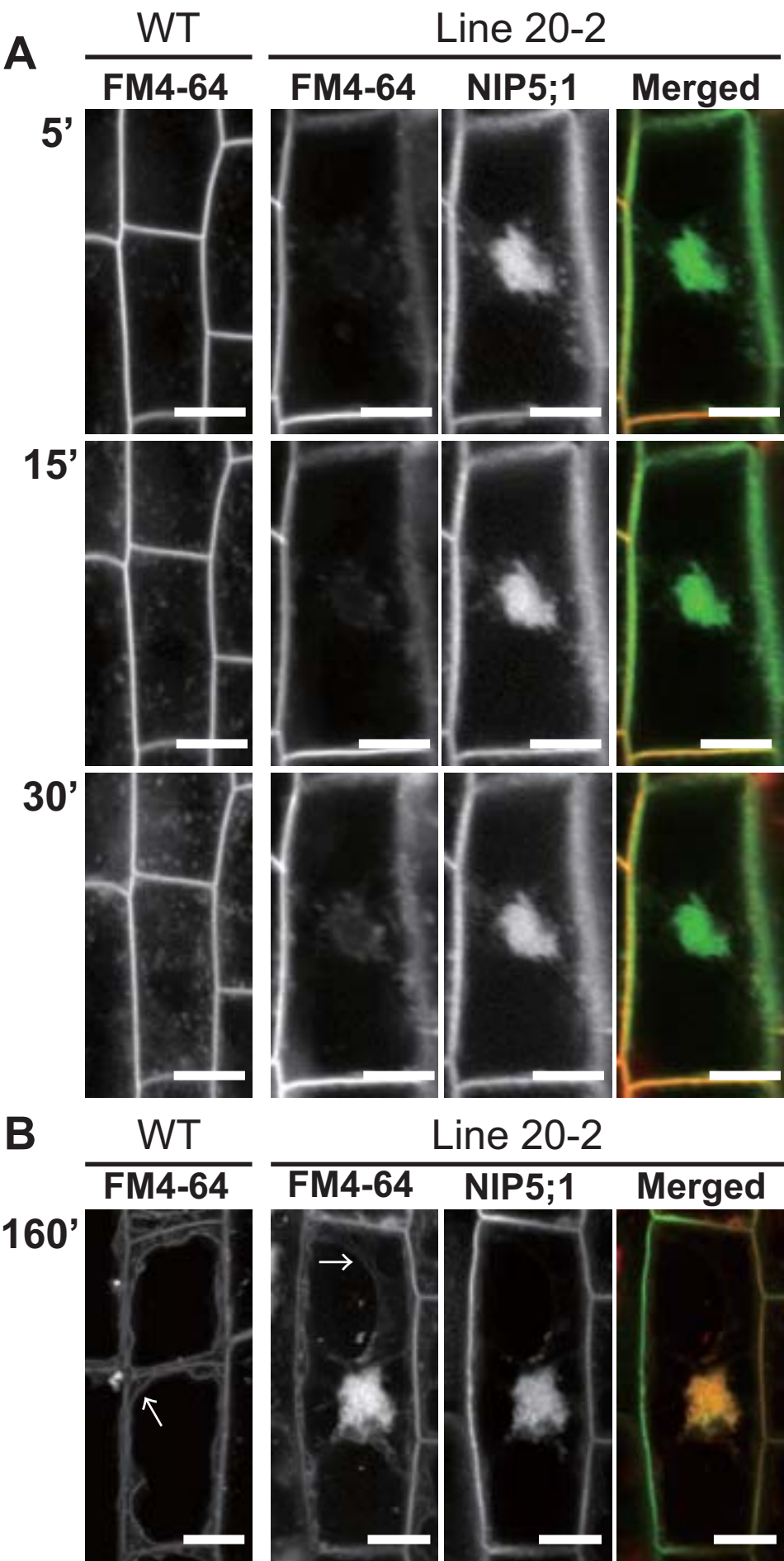
A
WT
Line 20-2
FM4-64
FM4-64
NIP5;1
Merged
5'
15'
30'
B
WT
Line 20-2
FM4-64
FM4-64
NIP5;1
Merged
160'

Fig. 5

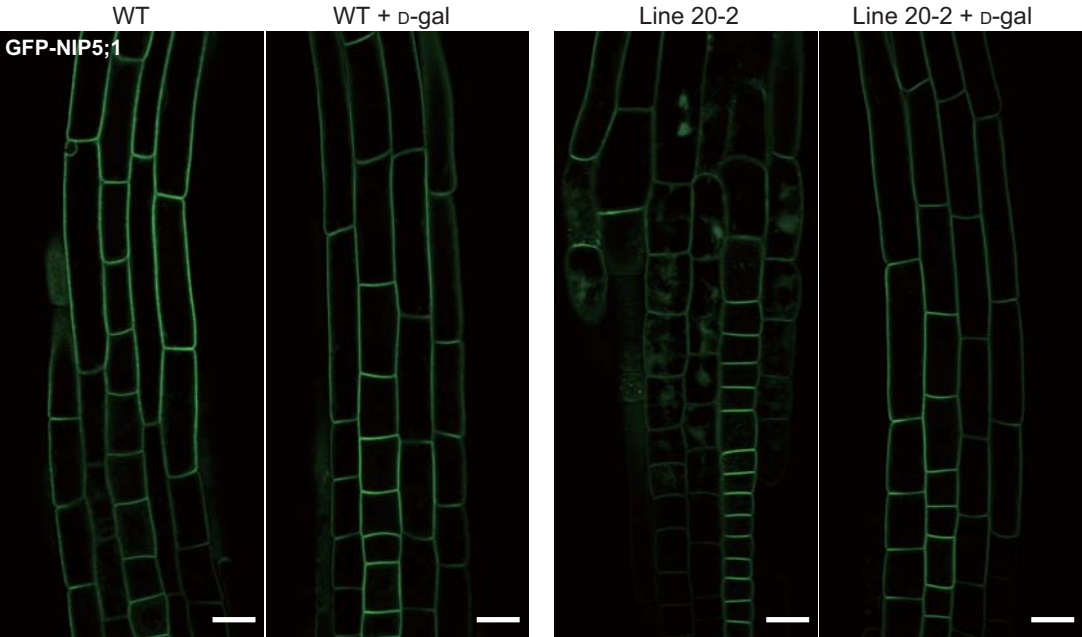

Fig. 6

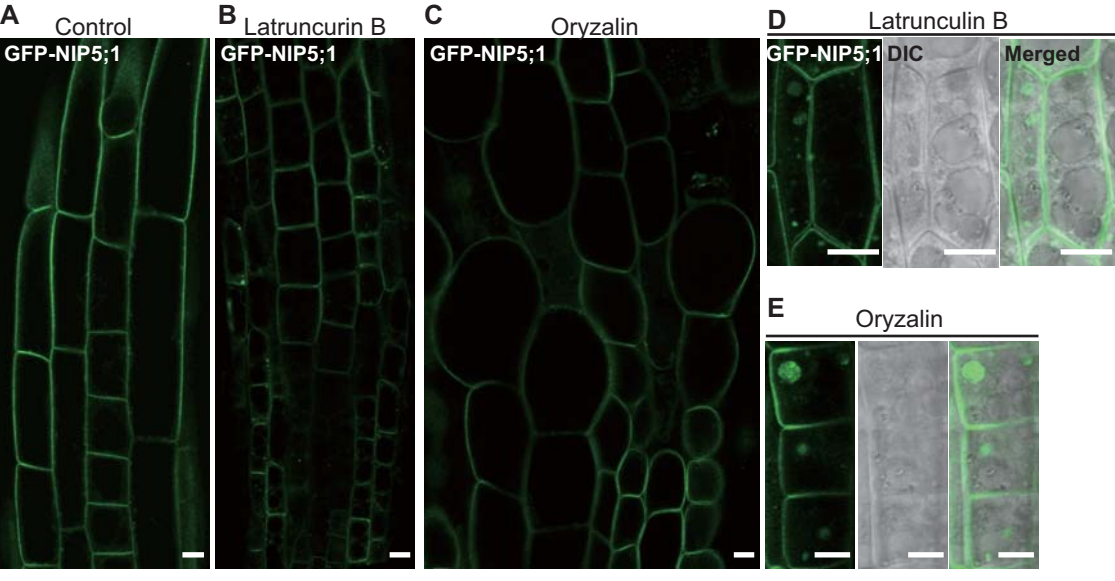
A
Control
GFP-NIP5;1
B
Latruncurin B
GFP-NIP5;1
C
Oryzalin
GFP-NIP5;1
D
Latrunculin B
GFP-NIP5;1
DIC
Merged
E
Oryzalin

Fig. 7

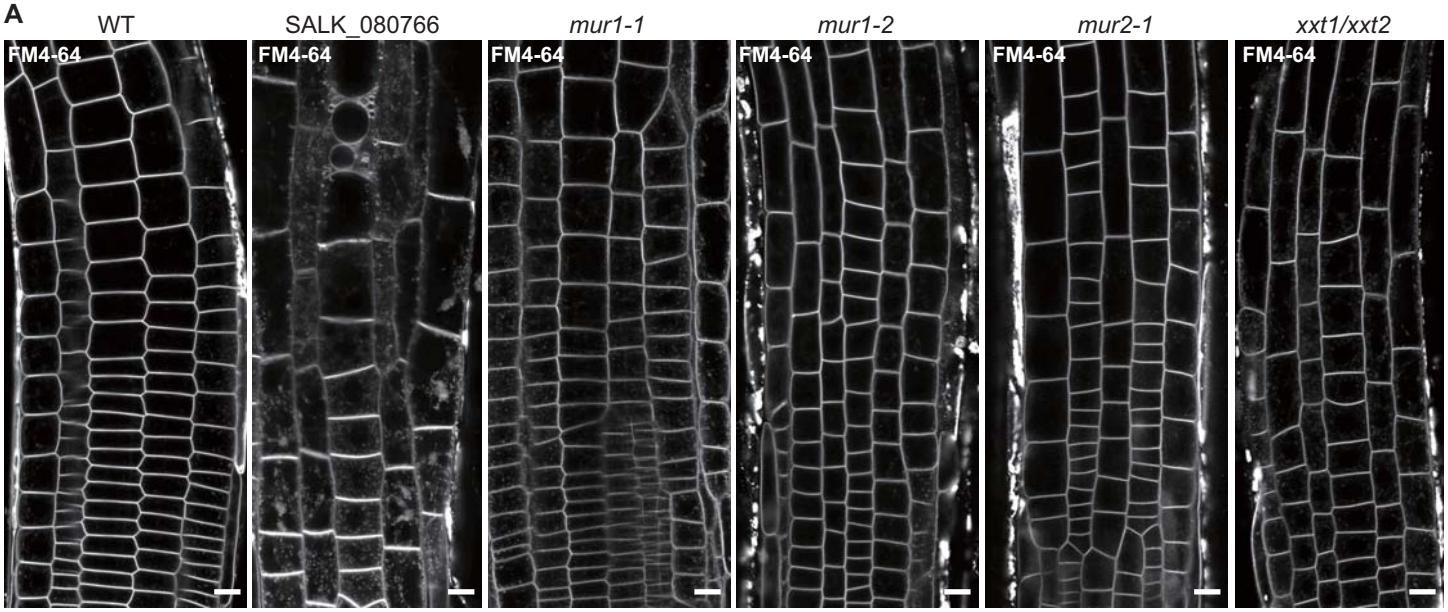
A
WT
SALK_080766
mur1-1
mur1-2
mur2-1
xxt1/xxt2
FM4-64
FM4-64
FM4-64
FM4-64
FM4-64
FM4-64

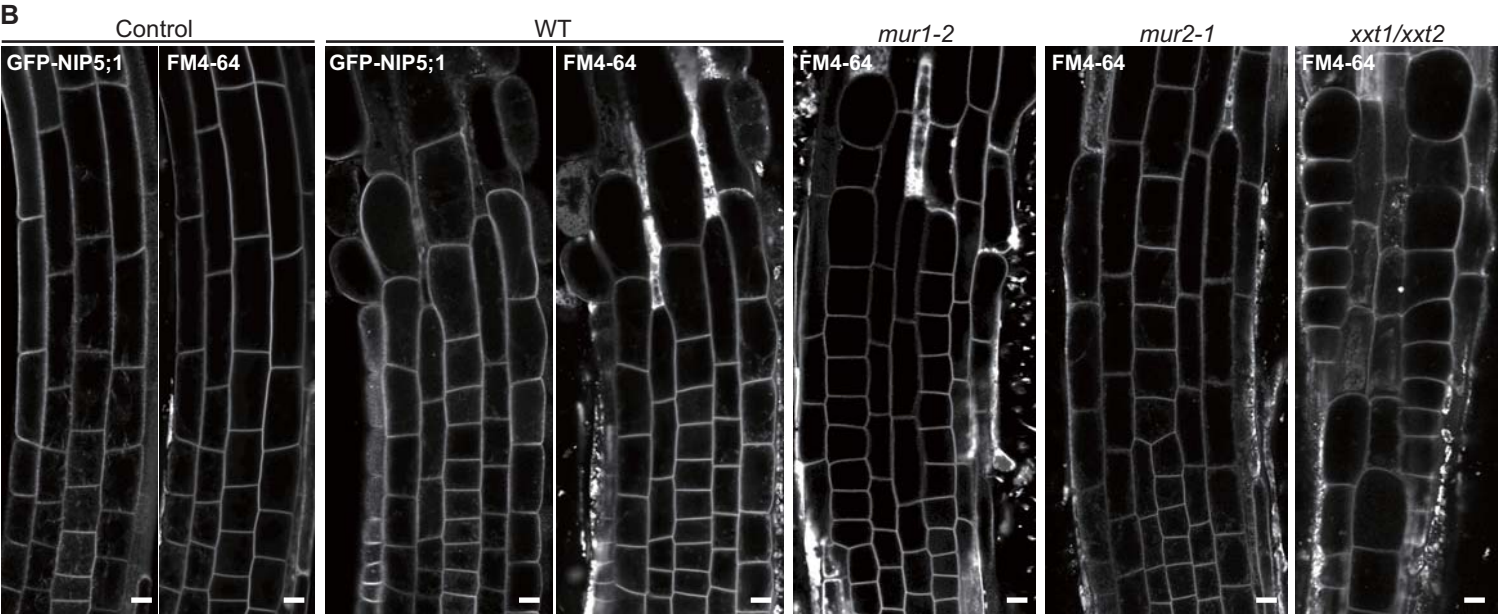
B
Control
WT
mur1-2
mur2-1
xxt1/xxt2
GFP-NIP5;1
FM4-64
GFP-NIP5;1
FM4-64
FM4-64
FM4-64
FM4-64

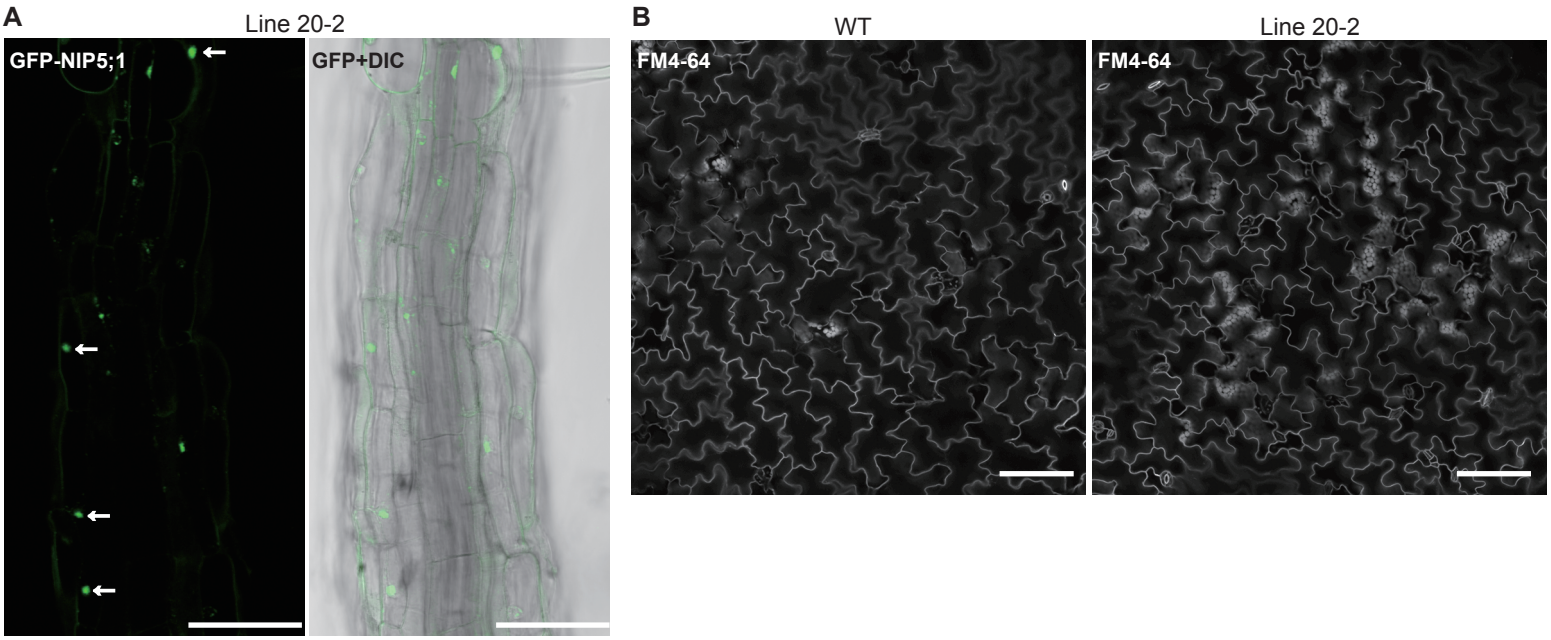

Supplementary Fig. S1

Aggregates were observed in epidermal cells in the root hair zone, but not in laeves, of Line 20-2. A) In epidermal cells of the root hair zone, GFP-NIP5;1 was localized in the aggregates. Note that the signal of GFP-NIP5;1 on the PM was low in this area. White arrows indicate the aggregates. B) No aggregate stained with FM4-64 in the epidermal cells of cotyledon in both the WT and Line 20-2. Plant leaves were stained with 4 μM FM4-64 for 30 min. Bars = 100 μm.

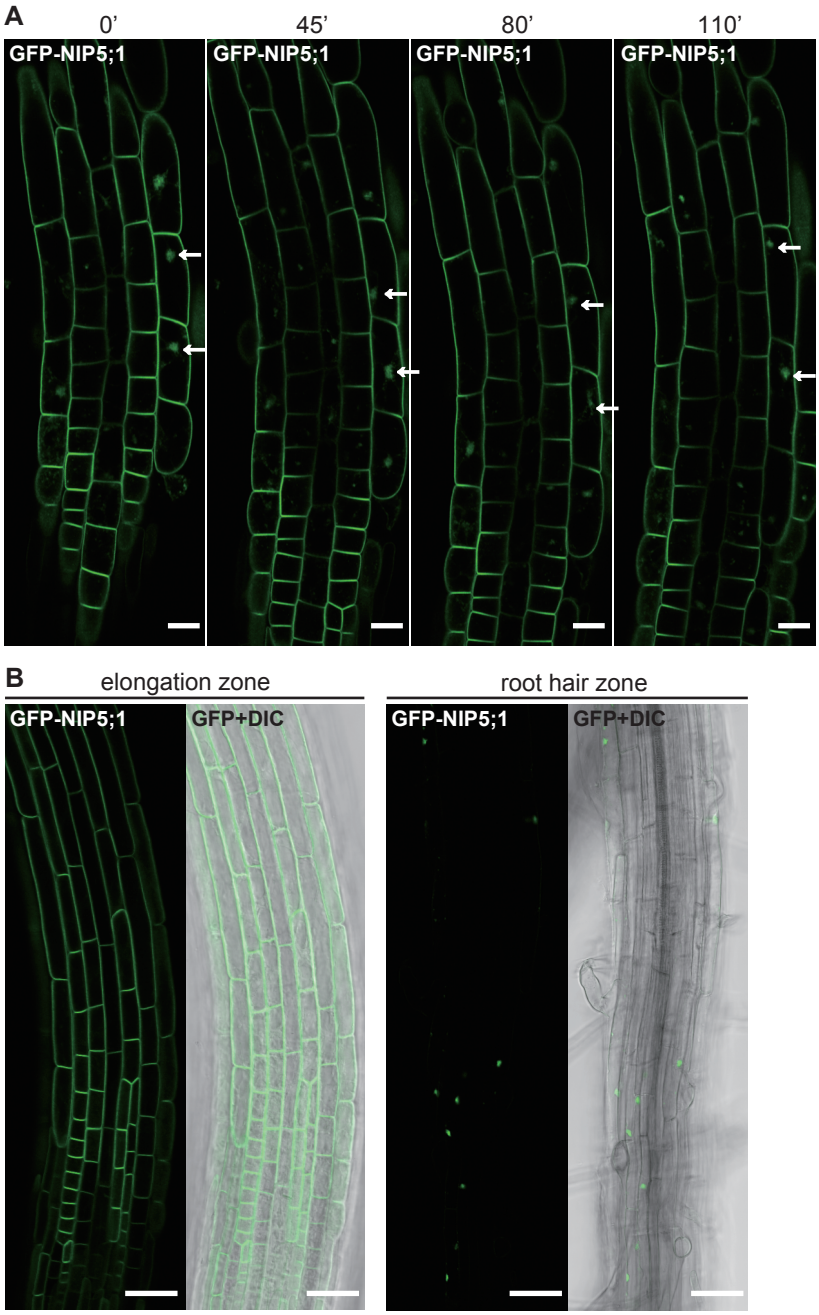

Supplementary Fig. S2
The presence of 10 mM D-galactose did not affect existing aggregates. (A) The aggregates (indicated by arrows) remained evident after 110 min. (B) The aggregates remained evident in epidermal cells in root hair zone, while they were not observed in the root elongation zone after 19 h in the presence of D-galactose. Bars = (A) 20 μm and (B) 50 μm.

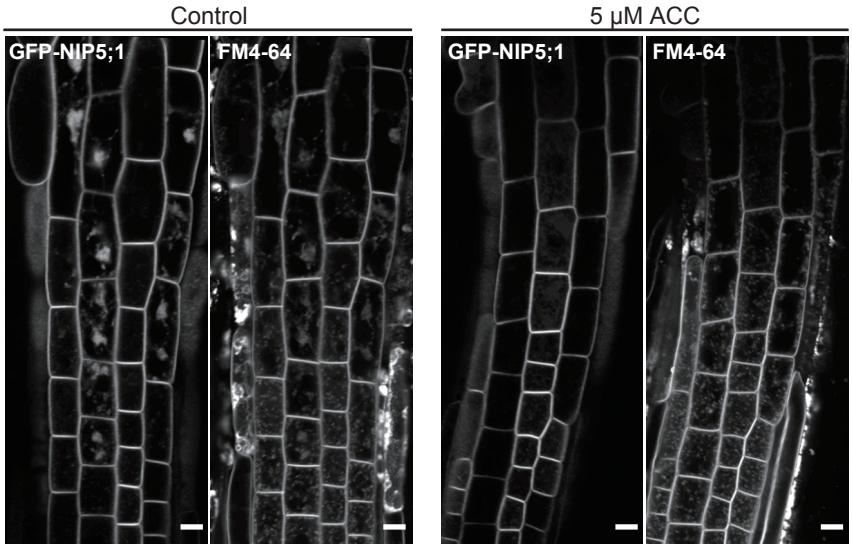

Supplementary Fig. S3

Ethylene precursor 1-aminocyclopropane-1-carboxylic acid (ACC) treatment rescued the aggregates. Five-day-old seedlings of Line 20-2 were transferred to solid medium containing 30 μM boric acid (Control) or 30 μM boric acid and 5 μM ACC for 2 days. Bars = 10 μm.

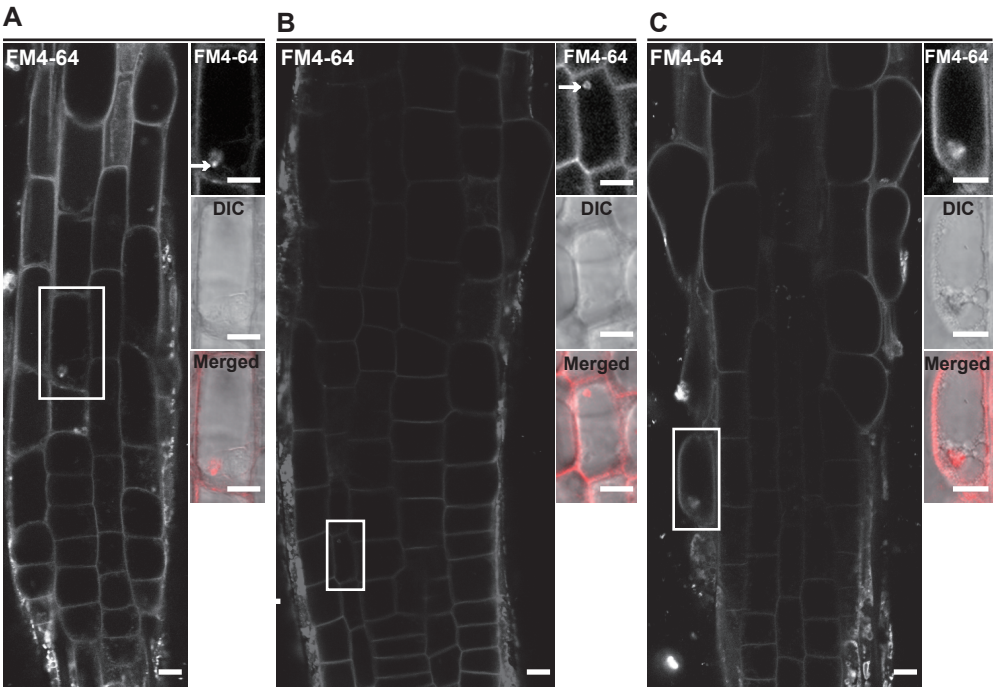

Supplementary Fig. S4

The abnormal structures were observed in some of the roots of the *xxt1/xxt2* mutant treated with Yariv reagent. The plants were treated with 30 μM β-D-glucosyl for 24 h and then stained with 4 μM FM4-64 for 30 min (A-C). Enlarged images with FM4-64 and DIC are shown in the right panels. In some of the abnormal structures, single spots with high intensity were observed (A and B, indicated by white arrows). Bars = 10 μm .

Supplementary Table S1: Primer sequences for rough mapping

Chromosome	Marker name	Location (Mb)	Forward (5'-3')	Reverse (5'-3')
1	F14J9	3.0	CGTGAACCCACTCGTTACATT	TGCATTTCAACTTTACCAACCA
	F28J9	13.8	ATGTTGGATTCAAGCACTTCC	AAGGTTCCGTCAGAGACGTG
	NGA 280	20.9	GGCTCCATAAAAAGTGCACC	CTGATCTCACGGACAATAGTGC
	NGA111	27.4	TGTTTTTTAGGACAAATGGCG	CTCCAGTTGGAAGCTAAAGGG
2	T12J2	3.5	ATCAACATCCGCAAAGTTCC	ACCTCCTTAGTCGCGTGAAA
	NGA168	16.3	GAGGACATGTATAGGAGCCTCG	TCGTCTACTGCACTGCCG
3	NGA162	4.6	CTCTGTCACTCTTTTCCTCTGG	CATGCAATTTGCATCTGAGG
	CIW4	18.9	GTTCATTAAACTTGCGTGTGT	TACGGTCAGATTGAGTGATTC
4	NGA8	5.6	TGGCTTTCGTTTATAAACATCC	GAGGGCAAATCTTTATTTCGG
5	MBK20	2.5	CCAAGACCAAAACCAAAACC	CATGCAATAGGCTTCGGAGT
	K20J1	19.9	TGACAACTTTGGGCAATTAAGA	CGCATGATGCATAGCAAAGT

Supplementary Table S2: List of candidate genes

Gene	SNP	Mutation	Protein (reference to TAIR)
AT1G56570	gGa=>gAa	G=>E	a mitochondria-localized pentatricopeptide repeat protein PGN
AT1G61310	Cag=>Aag	Q=>K	LRR and NB-ARC domains-containing disease resistance protein
AT1G64440	Gga=>Aga	G=>R	UDP-glucose 4-epimerase (AtUGE4/AtRHD1/AtREB1)
AT1G64780	Cag=>Tag	Q=>Stop	ammonium transporter 1;2
AT1G70340	Aga=>Tga	R=>Stop	unknown function
AT1G70580	ttG=>ttA	L=>L	glyoxylate aminotransferase
AT1G72390	aaG=>aaA	K=>K	unknown function
AT1G72950	gGt=>gAt	G=>D	Disease resistance protein (TIR-NBS class)
AT1G73160	Gag=>Aag	E=>K	UDP-Glycosyltransferase superfamily protein

Red letters mean non-EMS mutation.